組立てプロセス（３）　　電極分岐端子の接続と固定（表3-3, 3-4）

Auワイヤーは、10本のW鍼と電気的にそれぞれ独立接続される必要があるので、電極端子のNo.と鍼の関係が明確である必要がある。このため、Au線1本1本にNo札をつけ、電極端子に順番に接続される。また10本のAu線に伸縮性をもたせるために、Siチューブに螺旋状に巻き付け固定した。Siチューブは、鍼デバイス部のSiチューブと電極端子にしっかり接着固定される。詳細手順は表3-3及び3-4を参照。

表3-3　Auワイヤー処理その1

マウントベース治具に対し、Au線の末端を表3-4に示す手順で接続して行く。基本的にAgペーストで導通を取り、固定する方法は変わらない。最後にAu線を巻き付けているSiチューブとマウントベースを接着固定し、完成となる。

表3-4　Auワイヤー処理その2

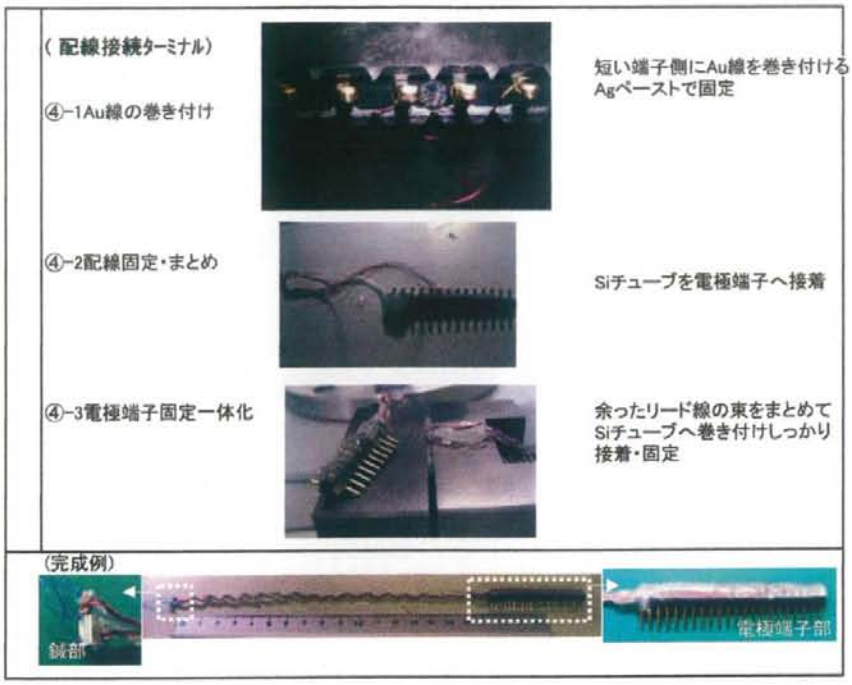

＜倫理面への配慮＞

本研究の動物実験は、国立循環器病センター研究所および日本生理学学会の動物実験の指針に沿い、実験動物の数と侵襲を最小にするよう、また、動物愛護上においても、十分配慮して行われた。また、国立循環器病センター研究所実験動物委員会に承認のもとに、行われた。

D．健康危険情報

健康危険情報は特にない。

E．研究発表

1．論文発表

Kamiya A, Kawada T, Mizuno M, Miyamoto T, Uemura K, Seki K, Shimizu S, Sugimachi M. Baroreflex increases correlation and coherence of muscle sympathetic nerve activity (SNA) with renal and cardiac SNAs. J Physiol Sci. 2006 Oct;56(5):325-33.

Kawada T, Miyamoto T, Miyoshi Y, Yamaguchi S, Tanabe Y, Kamiya A, Shishido T, Sugimachi M. Sympathetic Neural Regulation of Heart Rate is Robust Against High Plasma Catecholamines. J Physiol Sci. 2006 Jun;56(3):235-45.

Kawada T, Yamazaki T, Akiyama T, Uemura K, Kamiya A, Shishido T, Mori H, Sugimachi M. Effects of Ca2+ channel antagonists on nerve stimulation induced and ischemia-induced myocardial interstitial acetylcholine release in cats. Am J Physiol Heart Circ Physiol. 2006 Nov;291(5):H2187-91.

Aiba T, Shimizu W, Hidaka I, Uemura K, Noda T, Zheng C, Kamiya A, Inagaki M, Sugimachi M, Sunagawa K. Cellular basis for trigger and maintenance of ventricular fibrillation in the Brugada syndrome model: high-resolution optical mapping study. J Am Coll Cardiol. 2006 May 16;47(10):2074-85.

Michikami D, Kamiya A, Kawada T, Inagaki M, Shishido T, Yamamoto K, Ariumi H, Iwase S, Sugenoya J, Sunagawa K, Sugimachi M. Short-term electroacupuncture at Zusanli resets the arterial baroreflex neural arc toward lower sympathetic nerve activity. Am J Physiol Heart Circ Physiol. 2006 Jul;291(1):H318-26.

Uemura K, Kamiya A, Hidaka I, Kawada T, Shi mizu S, Shishido T, Yoshizawa M, Sugimachi M, Sunagawa K. Automated drug delivery system t o control systemic arterial pressure, cardiac outp ut, and left heart filling pressure in acute deco mpensated heart failure. J Appl Physiol. 2006 A pr;100(4):1278-86

Kawada T, Kitagawa H, Yamazaki T, Akiyam a T, Kamiya A, Uemura K, Mori H, Sugimach i M. Hypothermia reduces ischemia- and stim ulation-induced myocardial interstitial norepine phrine and acetylcholine releases J Appl Physi ol. 2007 Feb;102(2):622-7.

Uemura K, Li M, Tsutsumi T, Yamazaki T, Kawada T, Kamiya A, Inagaki M, Sunagawa K, Sugimachi M. Efferent vagal nerve stimulation induces tissue inhibitor of metalloproteinase-1 in myocardial ischemia-reperfusion injury in

rabbit. Am J Physiol Heart Circ Physiol. 2007 Oct;293(4):H2254-61. PMID: 17693545

Mizuno M, Kamiya A, Kawada T, Miyamoto T, Shimizu S, Sugimachi M. Muscarinic potassium channels augment dynamic and static heart rate Responses to vagal stimulation. Am J Physiol Heart Circ Physiol. 2007 Sep;293(3):H1564-70. PMID: 17526651

Nakaoka Y, Nishida K, Narimatsu M, Kamiya A, Minami T, Sawa H, Maeda M, Fujio Y, Koyama T, Yamasaki S, Sone M, Arai Y, Koh GY, Kodama T, Hirota H, Otsu K, Hirano T, Mochizuki N. Gab family scaffolding adaptor proteins are essential for the signal circuit between myocardium and endothelium. J Clin Invest 2007 Jul 2;117(7):1771-1781.

Kawada T, Kitagawa H, Yamazaki T, Akiyama T, Kamiya A, Uemura K, Mori H, Sugimachi M. Hypothermia reduces ischemia- and stimulation-induced myocardial interstitial norepinephrine and acetylcholine releases. J Appl Physiol. 2007 Feb;102(2):622-7. PMID: 17082372

Sugimachi M, Kawada T, Kamiya A, Li M, Zheng C, Sunagawa K. Electrical Acupuncture Modifies Autonomic Balance by Resetting the Neural Arc of Arterial Baroreflex System. Conf Proc IEEE Eng Med Biol Soc; 1: 5334-5337, 2007.

Kawada T, Shimuzu S, Yamamoto H, Shishido T, Kamiya A, Miyamoto T, Sunagawa K, Sugimachi M. Servo-Controlled Hind-Limb Electrical Stimulation for Short-Term Arterial Pressure Control. Circ J 2008 (in press)

Yamamoto H, Kawada T, Kamiya A, Kita T, Sugimachi M. Electroacupuncture changes the relationship between cardiac and renal sympathetic nerve activities in anesthetized cats. Auton Neurosci. 2008 Dec 15;144(1-2):43-9. PMID: 18990613

Mizuno M, Kamiya A, Kawada T, Miyamoto T, Shimizu S, Shishido T, Sugimachi M. Accentuated antagonism in vagal heart rate control mediated through muscarinic potassium channels. J Physiol Sci. 2008 Dec;58(6):381-8. PMID: 18842163

Miyamoto T, Kawada T, Yanagiya Y, Akiyama T, Kamiya A, Mizuno M, Takaki H, Sunagawa K, Sugimachi M.Contrasting effects of intrinsic operation and extrinsic activation of presynaptic {alpha}2-adrenergic inhibition on sympathetic heart rate control. Am J Physiol Heart Circ Physiol. 2008 Nov;295(5):H1855-66. PMID: 18757478

Yamamoto K, Kawada T, Kamiya A, Takaki H, Shishido T, Sunagawa K, Sugimachi M. Muscle mechanoreflex augments arterial baroreflex-mediated dynamic sympathetic response to carotid sinus pressure. Am J Physiol Heart Circ Physiol. 2008 Sep;295(3):H1081-H1089. PMID: 18586892

Kamiya A, Kawada T, Yamamoto K, Mizuno M, Shimizu S, Sugimachi M. Upright tilt resets dynamic transfer function of baroreflex neural

arc to minify the pressure disturbance in total baroreflex control. J Physiol Sci. 2008 Jun;58(3):189-98. PMID: 18471343

Kamiya A, Michikami D, Iwase S, Mano T. Decoding rule from vasoconstrictor skin sympathetic nerve activity to nonglabrous skin blood flow in humans at normothermic rest. Neurosci Lett. 2008 Jul 4;439(1):13-7. PMID: 18502048

2．学会発表

神谷　厚範、砂川　賢二、杉町　勝　生体信号を閉ループ制御するサーボ電気鍼システム　第45回日本生体医工学会大会　第44巻　110、2006

神谷　厚範、上村　和紀、清水　秀二、杉町　勝、砂川　賢二　宇宙心循環失調を克服する宇宙循環器医学の開発　第45回日本生体医工学会大会　第44巻　133、2006

上村　和紀、神谷　厚範、日高　一郎、川田　徹、清水　秀二、宍戸　稔聡、吉澤　誠、杉町　勝、砂川　賢二　急性重症心不全の循環管理を支援する血行動態自動制御システムの開発　第45回日本生体医工学会大会　第44巻　241、2006

藤崎　巌、川田　徹、高木　洋、砂川　賢二　高機能心拍制御機能を有したトレーニング機器の開発と実用化　第45回日本生体医工学会大会　第44巻　291、2006

宮本　忠吉、高木　洋、稲垣　正司、川田　徹、宍戸　稔聡、神谷　厚範、砂川　賢二、杉町　勝　心不全ラットにおける呼吸化学調節系の定量評価ー呼吸異常のメカニズム解明への解析的アプローチー　第45回日本生体医工学会大会　第44巻　545、2006

清水　秀二、宍戸　稔聡、上村　和紀、神谷　厚範、杉町　勝　右心低形成症候群に対する術式決定のためのシュミレーション　第45回日本生体医工学会大会　第44巻　546、2006

杉町　勝、上村　和紀、　神谷　厚範、李　梅花、鄭　燦、川田　徹　心不全の制御：急性心不全と慢性心不全の制御戦略　第27回日本循環制御医学会総会　循環制御 38，2006

宮本　忠吉、高木　洋、稲垣　正司、川田　徹、宍戸　稔聡、神谷　厚範、砂川　賢二、杉町　勝　心不全ラットにおける呼吸異常発生機構の解明ー統合的枠組みによる化学反射系の定量評価ー　第27回日本循環制御医学会総会　循環制御　55，2006

神谷　厚範、上村　和紀、清水　秀二、砂川　賢二、杉町　勝　心不全血行動態を自動治療する装置の開発：臨牀実用化へ向けて　第27回日本循環制御医学会総会　循環制御 63，2006

杉町　勝、川田　徹、神谷　厚範、宍戸　稔聡
Analysis of pressure regulatory system by control engineering approach　Neuroscience 2006 in Kyoto JAPAN　第２９回 日本神経科学大会 The 29th Annual Meeting of the Japan Neuroscience Society

UEMURA,KAZUNORI,Kamiya.Atsunori,Shimizu.shuji,Shishido.Toshiaki,Sugimachi.Masaru,Sunagawa.Kenji　Comprehensive Physiological Cardiovascular Model Enables Automatic Corrrection of Hemodynamics in Patients with Acute Life-Threatening Heart Failure, pp.198-201

IEEE EMBC 2006

Miyamoto.Tadayoshi,Inagaki.Masashi,Takaki.Hiroshi,Kamiya.Atsunori,Kawada.Toru,Shishido.Toshiaki,Sugimachi.Masaru,Sunagawa.Kenji Sensitized Central Controller of Ventilation in Rats with Chronic Heart Failure Contributes to Hyperpnea Little at Rest but More During Exercise, pp.4627-4630 IEEE EMBC 2006

Atsunori Kamiya, Kazunori Uemura, Shuji Shimizu,Masaru Sugimashi Kenji Sunagawa *A New Automated Drug Delivery System to Restore Hemodynamics of Decompensated Heart Failure in Closed-Chest Clinical Settings:Potential Application for Clinical Researchi* American Heart Association 2006

Yoshikazu Nakaoka, Atsunori Kamiya, Takashi Minami,Makiko Maeda, Yasushi Fujio, Tatsuya Koyama, Tatsuhiko Kodama, Hisao Hirota,Kinya Otsu,Naoki Mochizuki Gab Family Scaffolding Adaptor Proteins are Essential Mediators in the Signal Circuit between Myocardium and Endothelium The 71st Annual Scientific Metting of the Japanese Circulation Society

Taiki Higo, Rika Kawakami,Teruo Noguchi,Takahiro Ohara, Naohiko Aihara Noboru Oda, Hiroshi Takaki, Yoichi Goto *Effects of Exericise Cardiac Rehabilitation in Patients with Diastolic Heart failure after Acute Myocardial Infarction* The 71st Annual Scientific Metting of the Japanese Circulation Society

Kazunori Uemura, Meihua Li, Can Zheng, Toru Kawada, Masashi Inagaki, Atsunori Kamiya, Toji Yamazaki, Masaru Sugimachi Efferent Vagal Nerve Stimulation Suppresses Matrix Metalloproteinase Activity in Myocardial Ischemia-reperusion Injury in Rabbit The 71st Annual Scientific Metting of the Japanese Circulation Society

Tadayoshi Miyamoto, Hiroshi Takaki Masashi Inagaki, Toshiaki Shishido, Toru Kawada, Atsunori Kamiya, Kenji Sunagawa,Masaru Sugimachi *Central Chemoreflex Hypersensitivity in Rats with Chronic Heart Failure Contributes to Hyperphea Little at Rest but More during Exercise* The 71st Annual Scientific Metting of the Japanese Circulation Society

Dai Une Shuji Shimizu, Atsunori Kamiya, Kazunori Uemura, Toru Kawada, Toshiaki Shishido, Masaru Sugimachi Sympathetic Vasoconstriction Affects Graft Flow of Internal Thoracic Artery Only at Rest The 71st Annual Scientific Metting of the Japanese Circulation Society

Shuji Shimizu, Toshiaki Shishido, Kazunori Uemura, Atsunori Kamiya, Toru Kawada, Shunji Sano, Masaru Sugimachi We Should Assess the Physiological Characteristics of Hypoplastic Right Ventricle for Surgical Management of Pulmonary Atresia With Infact Ventricular Septum The 71st Annual Scientific Metting of the Japanese Circulation Society

水野　正樹、神谷　厚範、川田　徹、杉町　勝　Kachチャンネルは迷走神経性心拍反応を高速化し倍化する。　第84回日本生理学会大会　Program2007

神谷　厚範、上村　和紀、水野　正樹、清水　秀二、

杉町　勝　閉胸下臨床医学現場で、非代償性重症心不全の血行動態を管理する、新しい自動薬物治療装置第84回日本生理学会大会　Program2007

川田　徹、山崎　登自、秋山　剛、宍戸　稔聡、神谷　厚範、水野　正樹、杉町　勝アンジオテンシンⅡは迷走神経刺激時の心筋間質におけるアセチルコリン放出を抑制する。　第84回日本生理学会大会　Program2007

Shuji Smizu, Toshiaki Shishido, Kazunori Uemura, Atsunori Kamiya, Toru Kawada, Masaru Sugimachi New Physiological Classification for Surgical Management of Hypoplastic Right Ventricle in Pulmonary Atresia With Intact Ventricular Septum　56th Annual Scientific Session,ACC.07

川田　徹、山崎　登自、秋山　剛、宍戸　稔聡、神谷　厚範、水野　正樹、杉町　勝アンジオテンシンⅡは迷走神経刺激時の心筋間質におけるアセチルコリン放出を抑制する　第84回日本生理学会大会　Program2007

水野　正樹、神谷　厚範、川田　徹、杉町　勝　KAChチャンネルは迷走神経性心拍反応を高速化し倍化する　第84回日本生理学会大会　Program2007

神谷　厚範、上村　和紀、水野　正樹、清水　秀二、杉町　勝　閉胸下臨床医学現場で非代償性重症心不全の血行動態を管理する、新しい自動薬物治療装置第84回日本生理学会大会　Program2007

水野　正樹、神谷　厚範、川田　徹、杉町　勝　ムスカリン性K＋チャネルは迷走神経刺激に対する心拍応答を高速化し倍化する　第４６回日本生体工学会大会

清水　秀二、宍戸　稔聡、上村　和紀、神谷　厚範、杉町　勝　Norwood手術のシャント術式が心臓エナジェティクスに与える影響　第４６回日本生体工学会大会

宮本　忠吉、稲垣　正司、高木　洋、川田　徹、宍戸　稔聡、神谷　厚範、杉町　勝　　ヒト呼吸化学調節系の動特性の定量評価　第４６回日本生体工学会大会

上村　和紀、神谷　厚範、杉町　勝、砂川　賢二　血行動態自動制御システムによる心臓酸素効率最適化　第４６回日本生体工学会大会

神谷　厚範、上村　和紀、水野　正樹、清水　秀二、砂川　賢二　閉胸下臨床医学現で、非代償性重症心不全の血行動態を管理する、自動薬物治療装置　第４６回日本生体工学会大会

杉町　勝、李　梅花、鄭　燦、神谷　厚範、川田　徹　電気鍼による動脈圧反射系の修飾とその循環器疾患治療への応用　第４６回日本生体工学会大会

上村　和紀、神谷　厚範、杉町　勝、砂川　賢二　包括的循環平衡モデルの開発とその有用性　第２８回日本循環制御医学会総会

杉町　勝、上村　和紀、神谷　厚範、清水　秀二、宍戸　稔聡、砂川　賢二　包括循環平衡モデルに基づくバイオニック循環管理　第２８回日本循環制御医学会総会

T. Kawda, T.Miyamoto, M.Li, A.Kamiya and M.Sugimachi Dynamic characteristics of sympathetic nerve activity response to

Electroacupuncture at Zusanli in anesthetized cat. EXRERIMENTAL BIOLOGY 2007

M Sugimachi,T Kawada,A Kamiya,M Li,C Zheng,K Sunagawa Electrical Acupuncture Modifies Autonomic Balance by Resetting the Neural Arc of Arterial Baroreflex System. pp.5334-5337 IEEE EMB 2007

S Shimizu,T Shishido,K Uemura,A Kamiya,T Kawada,S Sano,M Sugimachi Right ventricle-pulmonary artery shunt for Norwood procedure is beveficial in reducing pressure-volume area and myocardial oxygen consumption compared to Blalock-Taussing Shunt:an in-silico analysis. European Society of Cardiology 2007

水野正樹、神谷厚範、川田徹、宍戸稔聡、杉町勝 ムスカリン性K+チャネルは交感神経緊張の有無に関わらず迷走神経刺激に対する動的及び静的心拍応答に貢献している 第85回日本生理学会総会

川田徹、水野正樹、神谷厚範、宍戸稔聡、杉町勝 血圧フィードバックによる電気鍼を用いた交感神経抑制システムの開発 第85回日本生理学会総会

M.Mizuno, A.Kamiya, T.Kawada and M.Sugimachi Muscarinic potassium channels play a significant role in the negative chronotropic response with or without background sympathetic tone. EXPERIMENTAL BIOLOGY 2008

神谷 厚範、杉町 勝 自律神経活動をモニター且つ刺激するマルチ電極MEMS神経装置の開発 第47回日本生体医工学会大会

水野 正樹、神谷 厚範、川田 徹、宍戸 稔聡、杉町 勝 交感神経緊張はムスカリンK+チャンネルによる徐脈作用の迅速性に影響を及ぼさない 第47回日本生体医工学会大会

清水 秀二、宍戸 稔聡、川田 徹、水野 正樹、日高 一郎、上村 和紀、神谷 厚範、杉町 勝 Ebstein奇形における右房化右室が２心室修復術後の心機能に与える影響 第47回日本生体医工学会大会

川田 徹、清水 秀二、水野 正樹、神谷 厚範、宍戸 稔聡、杉町 勝 血圧制御のための電気鍼の刺激強度調節システムの開発 第47回日本生体医工学会大会

M.Sugimachi, T.Kawada, H.Yamamoto, A.Kamiya, T.Miyamoto, K.Sunagawa Modification of Autonomic Balance by Electrical Acupuncture Does Not Affect Baroreflex Dynamic Characteristics 30th Annual International Conference of the IEEE Engineering in Medicine and Biology Society

M.Sugimachi, K.Uemura, T.Shishido, A.Kamiya, S.Shimizu, K.Sunagawa Theoretical and experimental demonstration of minumizing O2 consumption under preserved hemodynamics in heart failure XVIII th Cardiovascular System Dynamics Society

水野 正樹、川田 徹、神谷 厚範、宍戸 稔聡、杉町 勝．ラット交感および迷走神経刺激に対する動的心拍数応答．第101回近畿生理学談話会

清水　秀二、秋山　剛、川田　徹、水野　正樹、神谷　厚範、宍戸　稔聡、杉町　勝. 心臓マイクロダイアリシス法による心房アセチルコリン濃度の定量化. 第101回近畿生理学談話会

３．マスコミなどへの発表

日経ネットのニュース

神経刺激で心不全治療・国立循環器病センター研などが装置試作(2007/12/25)

http://health.nikkei.co.jp/news/med/index.cfm?i=2007122400667hb

Ｆ．知的財産権の出願・登録状況

4. 特許取得

【発明の名称】神経信号用プローバ、神経信号出力装置、神経信号記録装置、神経刺激装置及び神経信号入出力装置

【名称】神経信号用プローバ、神経信号出力装置、神経信号記録装置、神経刺激装置及び神経信号入出力装置

【発明者】神谷厚範、杉町　勝、桜井史敏、慶光院利映

【出願日】平成 19 年 2 月 1 日

【出願番号】特願 2007-023501

5. 実用新案登録

なし。

6. その他

なし

研究成果の刊行に関する一覧表

書籍

なし

雑誌

発表者氏名	論文タイトル名	発表誌名	巻号	ページ	出版年
Kamiya A, Kawada T, Mizuno M, Miyamoto T, Uemura K, Seki K, Shimizu S, Sugimachi M.	Baroreflex increases correlation and coherence of muscle sympathetic nerve activity (SNA) with renal and cardiac SNAs.	J Physiol Sci.	Oct;56(5)	325-33	2006
Kawada T, Miyamoto T, Miyoshi Y, Yamaguchi S, Tanabe Y, Kamiya A, Shishido T, Sugimachi M.	Sympathetic Neural Regulation of Heart Rate is Robust Against High Plasma Catecholamines.	J Physiol Sci.	Jun;56(3)	235-45	2006
Kawada T, Yamazaki T, Akiyama T, Uemura K, Kamiya A, Shishido T, Mori H, Sugimachi M.	Effects of Ca2+ channel antagonists on nerve stimulation induced and ischemia-induced myocardial interstitial acetylcholine release in cats.	J Physiol Heart Circ Physiol.	Nov;291 (5)	H2187 -91	2006
Aiba T, Shimizu W, Hidaka I, Uemura K, Noda T, Zheng C, Kamiya A, Inagaki M, Sugimachi M, Sunagawa K.	Cellular basis for trigger and maintenance of ventricular fibrillation in the Brugada syndrome model: high-resolution optical mapping study.	J Am Coll Cardiol.	May16; 47(10)	2074-85	2006
Michikami D, Kamiya A, Kawada T, Inagaki M, Shishido T, Yamamoto K, Ariumi H, Iwase S, Sugenoya J, Sunagawa K, Sugimachi M.	Short-term electroacupuncture at Zusanli resets the arterial baroreflex neural arc toward lower sympathetic nerve activity.	Am J Physiol Heart Circ Physiol.	Jul;291 (1)	H318-26	2006
Uemura K, Kamiya A, Hidaka I, Kawada T, Shimizu S, Shishido T, Yoshizawa M, Sugimachi M, Sunagawa K.	Automated drug delivery system to control systemic arterial pressure, cardiac output, and left heart filling pressure in acute decompensated heart failure.	J Appl Physiol.	Apr;100 (4)	1278-86	2006

Kawada T, Kitagawa H, Yamazaki T, Akiyama T, Kamiya A, Uemura K, Mori H, Sugimachi M.	Hypothermia reduces ischemia- and stimulation-induced myocardial interstitial norepinephrine and acetylcholine releases	J Appl Physiol.	Feb;102 (2)	622-7	2007
Uemura K, Li M, Tsutsumi T, Yamazaki T, Kawada T, Kamiya A, Inagaki M, Sunagawa K, Sugimachi M.	Efferent vagal nerve stimulation induces tissue inhibitor of metalloproteinase-1 in myocardial ischemia-reperfusion injury in rabbit.	Am J Physiol Heart Circ Physiol.	Oct;293 (4)	H2254-61	2007
Mizuno M, Kamiya A, Kawada T, Miyamoto T, Shimizu S, Sugimachi M.	Muscarinic potassium channels augment dynamic and static heart rate Responses to vagal stimulation.	Am J Physiol Heart Circ Physiol.	Sep;293 (3)	H1564-70	2007
Nakaoka Y, Nishida K, Narimatsu M, Kamiya A, Minami T, Sawa H, Maeda M, Fujio Y, Koyama T, Yamasaki S, Sone M, Arai Y, Koh GY, Kodama T, Hirota H, Otsu K, Hirano T, Mochizuki N.	Gab family scaffolding adaptor proteins are essential for the signal circuit between myocardium and endothelium.	J Clin Invest	Jul2;117 (7)	1771-1781	2007
Sugimachi M, Kawada T, Kamiya A, Li M, Zheng C, Sunagawa K.	Electrical Acupuncture Modifies Autonomic Balance by Resetting the Neural Arc of Arterial Baroreflex System.	Conf Proc IEEE Eng Med Biol Soc	1	5334-5337	2007
Kawada T, Shimuzu S, Yamamoto H, Shishido T, Kamiya A, Miyamoto T, Sunagawa K, Sugimachi M.	Servo-Controlled Hind-Limb Electrical Stimulation for Short-Term Arterial Pressure Control.	Circ J			in press
Yamamoto H, Kawada T, Kamiya A, Kita T, Sugimachi M.	Electroacupuncture changes the relationship between cardiac and renal sympathetic nerve activities in anesthetized cats.	Auton Neurosci	144	43-49	2008

Mizuno M, Kamiya A, Kawada T, Miyamoto T, Shimizu S, Shishido T, Sugimachi M.	Accentuated Antagonism in Vagal Heart Rate Control Mediated through Muscarinic Potassium Channels.	*J Physiol Sci*	58	381-388	2008
Miyamoto T, Kawada T, Yanagiya Y, Akiyama T, Kamiya A, Mizuno M, Takaki H, Sunagawa K, Sugimachi M.	Contrasting effects of presynaptic alpha2-adrenergic autoinhibition and pharmacologic augmentation of presynaptic inhibition on sympathetic heart rate control.	*Am J Physiol Heart Circ Physiol*	295	H1855-1866	2008
Yamamoto K, Kawada T, Kamiya A, Takaki H, Shishido T, Sunagawa K, Sugimachi M.	Muscle mechanoreflex augments arterial baroreflex-mediated dynamic sympathetic response to carotid sinus pressure.	*Am J Physiol Heart Circ Physiol*	295	H1081-H1089	2008
Kamiya A, Kawada T, Yamamoto K, Mizuno M, Shimizu S, Sugimachi M.	Upright tilt resets dynamic transfer function of baroreflex neural arc to minify the pressure disturbance in total baroreflex control.	*J Physiol Sci*	58	189-198	2008
Kamiya A, Michikami D, Iwase S, Mano T.	Decoding rule from vasoconstrictor skin sympathetic nerve activity to nonglabrous skin blood flow in humans at normothermic rest.	*Neurosci Lett.*	Jul 4; 439(1)	13-7	2008

REGULAR PAPER

J. Physiol. Sci. Vol. 56, No. 5 Oct. 2006; pp. 325–333
Online Sep. 9, 2006; **doi:10.2170/physiolsci.RP009006**

Baroreflex Increases Correlation and Coherence of Muscle Sympathetic Nerve Activity (SNA) with Renal and Cardiac SNAs

Atsunori KAMIYA, Toru KAWADA, Masaki MIZUNO, Tadayoshi MIYAMOTO, Kazunori UEMURA, Kenjiro SEKI, Shuji SHIMIZU, and Masaru SUGIMACHI

Department of Cardiovascular Dynamics, National Cardiovascular Centre Research Institute, Osaka, 565-8565 Japan

Reprinted from

The Journal of Physiological Sciences

Volume 56, Number 5, pp. 325–333, 2006
http://jphysiol.umin.jp doi:10.2170/physiolsci.RP009006

Published by The Physiological Society of Japan

Received on Jul 27, 2006; accepted on Sep 6, 2006; released online on Sep 9, 2006; doi:10.2170/physiolsci.RP009006
Correspondence should be addressed to: Atsunori Kamiya, Department of Cardiovascular Dynamics, National Cardiovascular Centre Research Institute, Osaka 565-8565, Japan. Tel: +81-6-6833-5012; Fax: +81-6-6835-5403; E-mail: kamiya@ri.ncvc.go.jp

J. Physiol. Sci. Vol. 56, No. 5; Oct. 2006; pp. 325–333
Online Sep. 9, 2006; **doi:10.2170/physiolsci.RP009006**

Baroreflex Increases Correlation and Coherence of Muscle Sympathetic Nerve Activity (SNA) with Renal and Cardiac SNAs

Atsunori KAMIYA, Toru KAWADA, Masaki MIZUNO, Tadayoshi MIYAMOTO, Kazunori UEMURA, Kenjiro SEKI, Shuji SHIMIZU, and Masaru SUGIMACHI
Department of Cardiovascular Dynamics, National Cardiovascular Centre Research Institute, Osaka, 565-8565 Japan

Abstract: Despite accumulating data of muscle sympathetic nerve activity (SNA) measured by human microneurography, whether neural discharges of muscle SNA correlates and coheres with those of other SNAs controlling visceral organs remains unclear. Further, how the baroreflex control of SNA affects the relations between these SNAs remains unknown. In urethane and α-chloralose anesthetized, vagotomized, and aortic-denervated rabbits, we recorded muscle SNA from the tibial nerve using microneurography and simultaneously recorded renal and cardiac SNAs. After isolating the carotid sinuses, we produced a baroreflex closed-loop condition by matching the isolated intracarotid sinus pressure (CSP) with systemic arterial pressure (CLOSE). We also fixed CSP at operating pressure (FIX) or altered CSP widely (WIDE: operating pressure ± 40 mmHg). Under these conditions, we calculated time-domain and frequency-domain measures of the correlation between muscle SNA and renal or cardiac SNAs. At CLOSE, muscle SNA resampled at 1 Hz correlated with both renal ($r^2 = 0.71 \pm 0.04$, delay = 0.10 ± 0.004 s) and cardiac SNAs ($r^2 = 0.58 \pm 0.03$, delay = 0.13 ± 0.004 s) at optimal delays. Moreover,muscle SNA at CLOSE strongly cohered with renal and cardiac SNAs(coherence >0.8) at the autospectral peak frequencies, and weakly (0.4–0.5) at the remaining frequencies. Increasing the magnitude of CSP change from FIX to CLOSE and further to WIDE resulted in corresponding increases in correlation and coherence functions at nonpeak frequencies, and the coherence functions at peak frequencies remained high (>0.8). In conclusion, muscle SNA correlates and coheres approximately with renal and cardiac SNAs under closed-loop baroreflex conditions. The arterial baroreflex is capable of potently homogenizing neural discharges of these SNAs by modulating SNA at the nonpeak frequencies of SNA autospectra.

Key words: sympathetic nerve activity, muscle, baroreflex.

Sympathetic nerve activity (SNA) has the crucial role of controlling circulation [1] and thus has been a major target in the research of circulatory physiology and pathophysiology. In humans, microneurography is the only direct method to measure SNA discharge [2]. By this technique, numerous human studies measured the activity of sympathetic nerves innervating the blood vessels in skeletal muscles (muscle SNA) [2–5] and used it as systemic SNA [3, 6–10]. However, since the measurable region in humans by this technique is almost limited to upper and lower extremities [2], the relation between muscle SNA and the SNAs controlling visceral organs such as the kidney and heart is not fully understood.

Arterial baroreflex is a major controller of SNA and thus may affect the relations between these SNAs. We previously reported that static-nonlinear and dynamic-linear baroreflex control of muscle SNA is similar to that of renal and cardiac SNAs under physiological pressure change in rabbits [11, 12]. Consistent with this finding, we have indeed observed that muscle SNA averaged over 1 minute parallels renal and cardiac SNAs in response to forced baroreceptor pressure change [11]. However, the relation between these SNAs in a time domain faster than 1 min and the relation in frequency domain remain unknown, despite the importance of their physiological and clinical relevance. First, the relation between these SNAs under conditions in which arterial pressure is regulated to normal level by a closed-loop baroreflex system is unclear. Next, the effects of baroreflex on the homogeneity in SNAs have not been analyzed quantitatively. Although canceling and enlarging the changes in baroreceptor pressure under open-loop baroreflex conditions are speculated to decrease and increase the homogeneity, respectively, how much muscle SNA correlates and coheres with other SNAs under these conditions remains unknown.

In the present study, we tested two hypotheses: (i) muscle SNA correlates and coheres with renal and cardiac SNAs under a closed-loop baroreflex condition, and (ii) the arterial baroreflex is capable of homogenizing neural discharges of these SNAs. In anesthetized rabbits with ca-

Received on Jul 27, 2006; accepted on Sep 6, 2006; released online on Sep 9, 2006; doi:10.2170/physiolsci.RP009006
Correspondence should be addressed to: Atsunori Kamiya, Department of Cardiovascular Dynamics, National Cardiovascular Centre Research Institute, Osaka 565-8565, Japan. Tel: +81-6-6833-5012; Fax: +81-6-6835-5403; E-mail: kamiya@ri.ncvc.go.jp

rotid sinuses isolated from systemic circulation, we simultaneously recorded muscle SNA from the tibial nerve by microneurography as well as renal and cardiac SNAs. We investigated the relation of muscle SNA with renal and cardiac SNAs under closed-loop baroreflex conditions and determined the proportions of the variance components of muscle SNA correlating and not correlating with renal and cardiac SNAs. Further, we also investigated these relations under two open-loop baroreflex conditions: fixed and widely fluctuating baroreceptor pressure.

MATERIALS AND METHODS

Surgical preparations. The animals were cared for in strict accordance with the Guiding Principles for the Care and Use of Animals in the Field of Physiological Sciences approved by the Physiological Society of Japan. Ten Japanese white rabbits weighing 2.4–3.3 kg were anesthetized by intravenous injection (2 ml/kg) of a mixture of urethane (250 mg/ml) and α-chloralose (40 mg/ml) and mechanically ventilated with oxygen-enriched room air. Supplemental anesthetics were injected as necessary (0.5 ml/kg) to maintain an appropriate level of anesthesia. We isolated the bilateral carotid sinuses vascularly from the systemic circulation by ligating the internal and external carotid arteries and other small branches originating from the carotid sinus regions. The isolated carotid sinuses were filled with warmed physiological saline through catheters inserted via the common carotid arteries. The intracarotid sinus pressure (CSP) was controlled by a servo-controlled piston pump (model ET-126A, Labworks; Costa Mesa, CA). Bilateral vagal and aortic depressor nerves were sectioned at the midlevel of the neck to eliminate baroreflexes from the cardiopulmonary region and the aortic arch. The systemic arterial pressure (AP) was measured using a high-fidelity pressure transducer (Millar Instruments; Houston, TX) inserted retrograde from the right common carotid artery below the isolated carotid sinus region. Body temperature was maintained at approximately 38°C with a heating pad.

We exposed the left renal sympathetic nerve retroperitoneally and the left cardiac sympathetic nerve through a middle thoracotomy. We attached a pair of stainless steel wire electrodes (Bioflex wire AS633, Cooner Wire) to each of these nerves to record renal and cardiac SNAs. To eliminate afferent signals, we tightly ligated and crushed the nerve fibers peripheral to the electrodes. To insulate and fix the electrodes, we covered the nerve and electrodes with a mixture of silicone gel (Silicon Low Viscosity, KWIK-SIL, World Precision Instrument, Inc., FL). We band-pass filtered the preamplified nerve signals at 150–1,000 Hz.

We exposed the left tibial nerve at the right popliteal fossa by incising the flexors of the dorsal middle thigh. We inserted a tungsten microelectrode (model 26-05-1, Federick Haer and Co., Bowdoinham, ME) to the right tibial nerve to record muscle SNA according to the microneurographic technique reported in humans [2, 13] and animals [14]. We identified muscle SNA according to the following discharge characteristics: (i) afferent activity being induced by tapping of the calf muscles but not by gently touching the skin, and (ii) excitatory and inhibitory responses to decreasing and increasing CSP, respectively. Then we tightly ligated and crushed the nerve fibers peripheral to the electrodes to eliminate afferent signals from the muscles. We fed the nerve signals into a preamplifier (Kohno Instruments, Nagoya) with active band-pass filters set from 480 to 5,000 Hz and continuously monitored these signals through a sound speaker.

We full-wave rectified and low-pass filtered the SNA signals with a cutoff frequency of 30 Hz to quantify the nerve activity. Pancuronium bromide (0.1 mg/kg) was administrated to prevent a contamination of muscular activity in these SNA recordings.

Protocols. After the surgical preparation, we kept the animal horizontally in a supine position. To test the first hypothesis that a neural discharge of muscle SNA parallels that of renal and cardiac SNAs, we measured the three SNAs while closing the baroreflex negative feedback loop by matching CSP with systemic AP (CLOSE protocol). We recorded CSP, SNAs, and systemic AP for 15 min at a sampling rate of 200 Hz, using a 12-bit analog-to-digital converter. After stabilizing the condition for at least 5 min, we recorded the data for 10 min and stored them on the hard disk of a dedicated laboratory computer system for later analysis. We also calculated the actual operating pressure by averaging systemic AP from the data.

To test the second hypothesis that baroreflex contributes to homogeneous sympathetic activation, we eliminated and greatly widened the baroreceptor pressure changes by the FIX and WIDE protocols, respectively, in baroreflex open-loop conditions. In the FIX protocol, we fixed CSP at the operating pressure [15, 16]. In the WIDE protocol, we randomly assigned CSP at 40 mmHg either above or below the operating pressure every 500 ms according to a binary white noise sequence [15, 17], where the input power spectrum of CSP was reasonably flat up to 1 Hz. The FIX and WIDE protocols were conducted serially in a randomized order at intervals of at least 5 min between protocols. During each protocol, we recorded measurements for 10 min and stored the data for analysis.

Data analysis. Under each baroreceptor pressure condition of CLOSE, WIDE, and FIX, we calculated the time domain (correlation coefficient) and frequency domain measures (coherence function) between muscle and renal or cardiac SNAs. In the time-domain analysis, we resampled SNA data at 1 Hz, assigned 100 arbitrary units (a.u.) to the maximal value during 10 min of CLOSE, and normalized other SNA signals to this value.

We scatter-plotted muscle SNA at 1 Hz against renal and cardiac SNAs with variable delays from renal and cardiac SNAs to muscle SNA (range: from 0 to 0.30 s at increments of 0.01 s) and calculated the correlation coefficient (r) [18] with optimal delays that maximized the square of correlation coefficient (r^2). The delays reflected the distances from the brain to the sites of measurement of these SNAs. The r^2 shows how perfectly a linear regression line describes the relationship between the two SNAs [19].

We also calculated the variance of muscle SNA resampled at 1 Hz [19]. The variance may include two components, one that correlates (correlative variance) and the other that does not correlate (noncorrelative variance) with other SNAs. Therefore we defined correlative and noncorrelative variance of muscle SNA to renal or cardiac SNA as follows (see APPENDIX) [18, 19]:

Correlative variance = SNA variance·r^2
Noncorrelative variance = SNA variance·$(1 - r^2)$

where SNA variance was the variance of muscle SNA, and r^2 was the correlation coefficient of muscle SNA against renal or cardiac SNA.

In the frequency-domain analysis, we calculated the coherence functions between muscle SNA and renal or cardiac SNA. We resampled SNA data at 10 Hz, and segmented them into 10 sets of 50% overlapping bins of 2^{10} data point each. SNA signals were similarly normalized as mentioned above. The segment length was 102.4 s, which yields the lowest frequency bound of 0.01 (0.0097) Hz. For each data set, we performed a fast Fourier transform while subtracting a linear trend and applying a Hanning window for each segment. We performed fast Fourier transform and ensemble averaged the power of muscle SNA [$S_{xx}(f)$], the power of renal or cardiac SNA [$S_{yy}(f)$], and the cross power between muscle SNA and renal or cardiac SNA [$S_{yx}(f)$] over the 10 segments. We derived a magnitude-squared coherence function [$Coh(f)$] of muscle SNA versus renal and cardiac SNAs as follows [17]:

$$Coh(f) = \frac{|S_{yx}(f)|^2}{S_{xx}(f)S_{yy}(f)}$$

The coherence value ranges from zero to unity. Unity coherence indicates a perfect linear correlation between muscle SNA and other SNAs, whereas zero coherence indicates total independence of the two SNAs. In an SNA autospectrum, when the power was three times greater than the averaged power of SNA from 0.01 to 1 Hz, we defined it as a peak. We separately calculated the averaged coherence function at the peak frequencies of muscle SNA autospectra and that at the remaining frequencies.

Statistic analysis. We presented all data as means ± SD. We used a repeated-measures analysis of variance with post hoc multiple comparisons to compare variables among experimental baroreceptor pressure conditions (FIX, CLOSE, WIDE) [19]. We considered differences significant when $P < 0.05$.

RESULTS

Relation between muscle SNA and cardiac or renal SNA in closed-loop baroreflex condition of CLOSE protocol

Time-domain analysis. In the CLOSE protocol (CSP matched with systemic arterial pressure), typical neural discharges of muscle SNA at 10 Hz appeared roughly the same as those of renal and cardiac SNAs (Fig. 1A). When the delay from renal and cardiac SNAs to muscle SNA was determined in individual animals to maximize r^2 (a typical example is shown in Fig. 1), muscle SNA resampled at 1 Hz correlated with both renal and cardiac SNAs with r^2 of 0.81 (delay = 0.10 s) and 0.64 (delay = 0.13 s), respectively (Fig. 1, B and C). The averaged data of all animals also showed that muscle SNA correlated with renal SNA ($r^2 = 0.71 \pm 0.04$, delay = 0.10 ± 0.004 s) and with

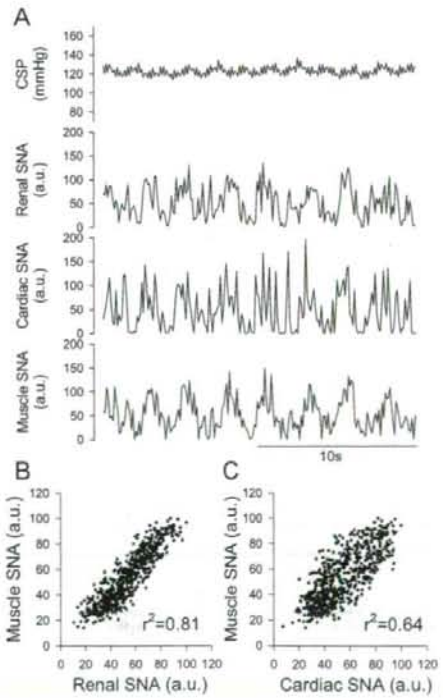

Fig. 1. (**A**) Representative time series for CSP, renal, cardiac, and muscle SNAs resampled at 10 Hz under the baroreflex closed-loop condition of CLOSE (CSP was matched to systemic AP). (**B**) Scatter plot of muscle SNA against renal SNA. (**C**) Scatter plot of muscle SNA against cardiac SNAs. The SNA signals were further resampled at 1 Hz. The delay from renal (0.10 s) or cardiac SNA (0.13 s) to muscle SNA was determined as the value that maximized r^2.

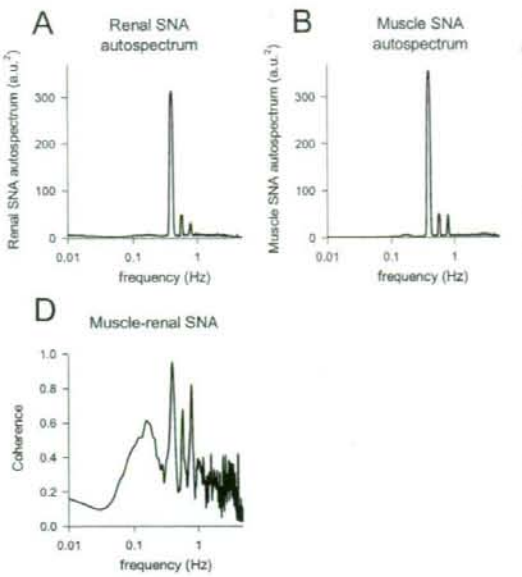

Fig. 2. Autospectra of renal (**A**), muscle (**B**), and cardiac SNAs (**C**) resampled at 1 Hz, and the coherence function of muscle SNA against renal (**D**) and cardiac SNAs (**E**) under the baroreflex closed-loop condition of CLOSE (CSP was matched to systemic AP), using the same data as in Fig. 1.

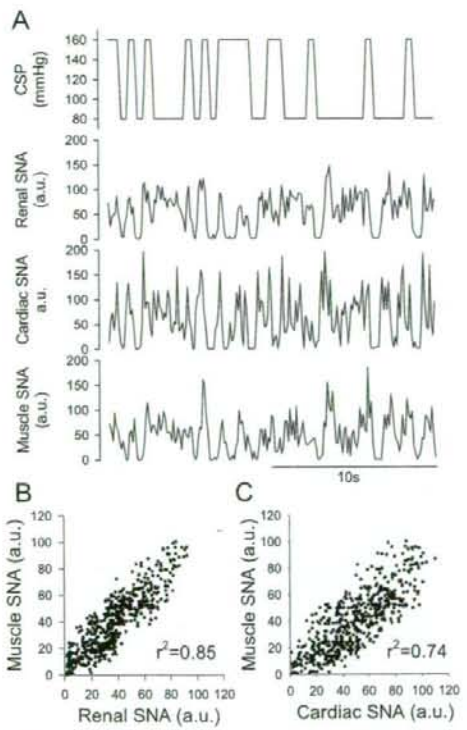

Fig. 3. (**A**) Representative time series for CSP, renal, cardiac, and muscle SNAs resampled at 10 Hz under the baroreflex open-loop condition of WIDE (CSP was varied according to a binary white noise sequence at 40 mmHg either above or below the operating pressure). (**B**) Scatter plots of muscle SNA resampled at 1 Hz against renal SNA (delay = 0.10 s). (**C**) Scatter plots of muscle SNA resampled at 1 Hz against cardiac SNA (delay = 0.13 s).

cardiac SNA ($r^2 = 0.58 \pm 0.03$, delay = 0.13 ± 0.004 s) (Fig. 5, A and B). The r^2 was greater with renal than with cardiac SNA ($P < 0.05$). The pulse pressure of CSP was 30–40 mmHg.

Frequency-domain analysis. In the same animal as in Fig. 1, the autospectra of these SNAs showed a few peaks at common frequency ranges (Fig. 2, A, B, and C). Muscle SNA cohered with both renal and cardiac SNAs strongly at the peak frequencies of muscle SNA autospectra, but weakly at the remaining frequencies (Fig. 2, D and E). The individual animals all showed similar characteristics. The averaged coherence function of the animals was strong at the peak frequencies of the muscle SNA autospectrum (0.93 ± 0.01 between muscle and renal SNAs and 0.87 ± 0.02 between muscle and cardiac SNAs), but was weak at the remaining frequencies (0.5) (Fig. 8).

Effects of the magnitude of change in baroreceptor pressure on the relation between muscle SNA and cardiac or renal SNA

Time-domain analysis. In the same animal as in Fig. 1, the pattern of neural discharge of muscle SNA at 10 Hz resembled those of renal and cardiac SNAs to a greater extent in the WIDE protocol (CPS fluctuating between operating pressure ± 40 mmHg) (Fig. 3) than in the FIX protocol (CPS fixed at operating pressure) (Fig. 4). The correlation of muscle SNA resampled at 1 Hz with renal and cardiac SNAs was higher in WIDE ($r^2 = 0.85$, delay = 0.10 s, and $r^2 = 0.74$, delay = 0.13 s, respectively) (Fig. 3, B and C) than in CLOSE, but was lower in FIX (with the same delays, Fig. 4, B and C). Compared with CLOSE, the averaged data of all animals showed a higher correlation of muscle SNA with renal and cardiac SNAs in WIDE ($r^2 = 0.79 \pm 0.03$, delay = 0.10 ± 0.004 s, and $r^2 =$

0.76 ± 0.02, delay = 0.13 ± 0.004 s, respectively), but lower correlation in FIX ($r^2 = 0.53 \pm 0.04$, delay = 0.10 ± 0.004 s, and $r^2 = 0.46 \pm 0.04$, delay = 0.13 ± 0.004 s, respectively) (Fig. 5, A and B). In WIDE, the r^2 was higher with renal than with cardiac SNA ($P < 0.05$). Similar results were observed when SNAs were resampled at slower and faster frequencies than 1 Hz (Fig. 6). In both SNA pairs, the r^2 was greater in WIDE than in CLOSE and FIX at frequencies from 0.01 to 5 Hz ($P < 0.05$), whereas it was greater in CLOSE than in FIX at frequencies from 0.3 to 5 Hz ($P < 0.05$).

The variance of muscle SNA sampled at 1 Hz increased from FIX to CLOSE and further to WIDE (Fig. 5, C and D; gray plus black column). The variance component of

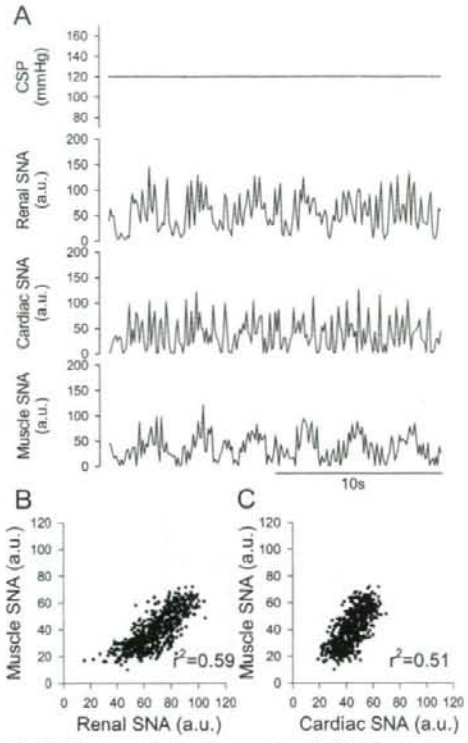

Fig. 4. (**A**) Representative time series for CSP, renal, cardiac, and muscle SNAs resampled at 10 Hz under the baroreflex open-loop condition of FIX (CSP was fixed at the operating pressure). (**B**) Scatter plot of muscle SNA resampled at 1 Hz against renal SNA (delay = 0.10 s). (**C**) Scatter plots of muscle SNA resampled at 1 Hz against cardiac SNA (delay = 0.13 s).

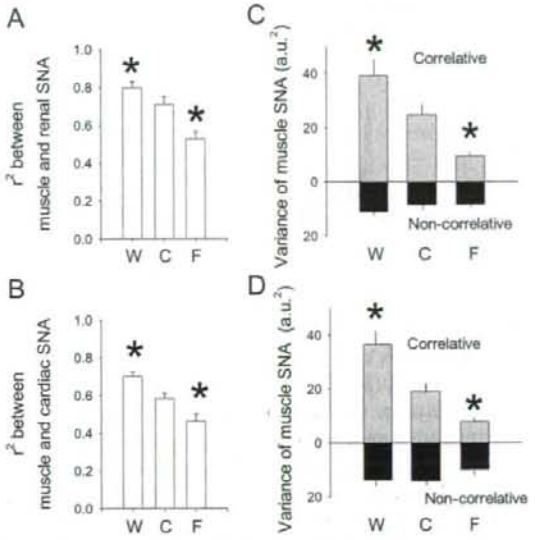

Fig. 5. The square of correlation coefficient (r^2) between muscle SNA resampled at 1 Hz and renal (**A**) or cardiac SNA (**B**) under baroreceptor pressure conditions of WIDE, CLOSE, and FIX. Floating columns show the averaged (±SD) correlative (gray top column) and noncorrelative (black bottom column) variance of muscle SNA versus renal (**C**) or cardiac SNA (**D**) resampled at 1 Hz in WIDE, CLOSE, and FIX. Correlative: variance component of muscle SNA correlating with other SNA; Noncorrelative: variance component of muscle SNA not correlating with other SNA; W: WIDE; C: CLOSE; F: FIX. *: $P < 0.05$, vs. CLOSE.

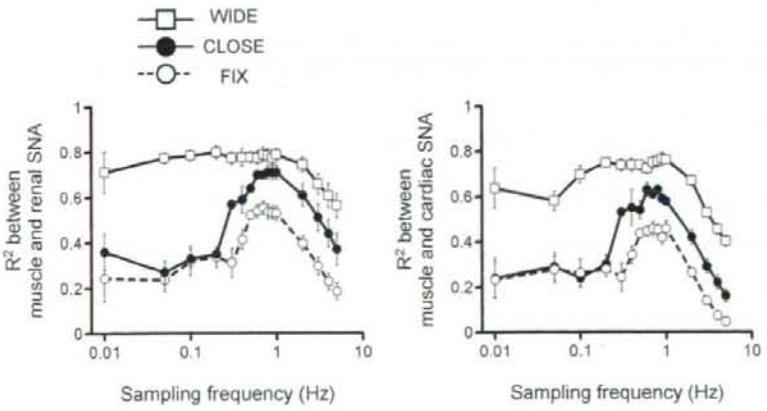

Fig. 6. The square of correlation coefficient (r^2) over SNA sampling frequency (0.01–5.0 Hz) between muscle SNA and renal (**A**) or cardiac SNA (**B**) under baroreceptor pressure conditions of WIDE (open square), CLOSE (closed circle), and FIX (open circle). In both SNA pairs, the r^2 was greater in WIDE than in CLOSE and FIX at frequencies observed ($P < 0.05$), whereas it was greater in CLOSE than in FIX at frequencies from 0.3 to 5.0 Hz ($P < 0.05$).

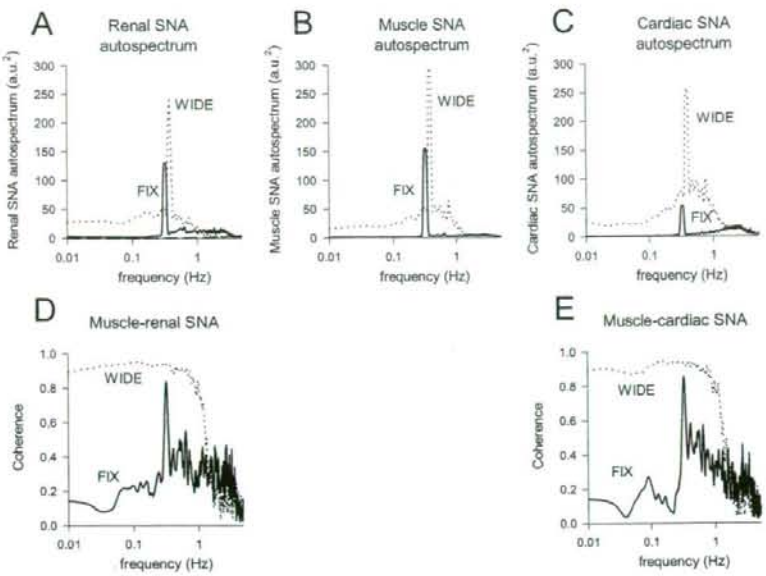

Fig. 7. Autospectra of renal (**A**), muscle (**B**), and cardiac SNAs (**C**), and the coherence function of muscle SNA against renal (**D**) and cardiac SNAs (**E**) under baroreflex open-loop conditions of WIDE (broken line) and FIX (solid line), using the same data as in Figs. 3 and 4.

muscle SNA that correlates with other SNAs, calculated as muscle SNA variance·r^2 ranked in the order of WIDE > CLOSE > FIX (Fig. 5, C and D; gray column), indicating a contribution of baroreflex-dependent regulation in maintaining homogeneity between muscle SNA and other visceral SNAs. In contrast, the variance component of muscle SNA that does not correlate with other SNAs, calculated as variance · $(1 - r^2)$, was similar among FIX, CLOSE, and WIDE (Fig. 5, C, D; black bottom column).

Frequency-domain analysis. In the same animal as in Fig. 1, the autospectra of muscle, renal, and cardiac SNAs peaked at exactly the same frequencies both in the WIDE and FIX protocols (Fig. 7, A, B, and C). Muscle SNA strongly cohered with both renal and cardiac SNAs both in WIDE and FIX at peak frequencies of the muscle SNA autospectra; however, the correlation was strong in WIDE but weak in FIX at the remaining frequencies (Fig. 7, D and E). The data of individual animals showed similar characteristics. The averaged coherence functions of all animals was consistently strong (>0.8) at peak frequencies of the muscle SNA autospectra regardless of baroreceptor pressure conditions of WIDE, CLOSE, and FIX (Fig. 8, black column). In contrast, the averaged coherence functions at the remaining frequencies were higher in WIDE (>0.8) compared with CLOSE or FIX (0.4–0.5) (Fig. 8, gray column).

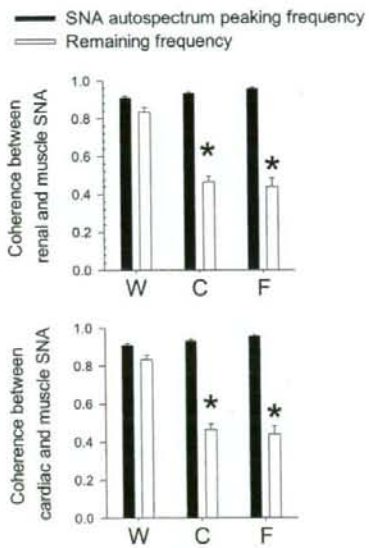

Fig. 8. Averaged coherence functions of muscle SNA against renal and cardiac SNAs at muscle SNA autospectral peak frequencies (black column) and at the remaining frequencies (gray column) under baroreceptor pressure conditions of WIDE, CLOSE, and FIX. W: WIDE; C: CLOSE; F: FIX. *P < 0.05, WIDE vs. CLOSE and FIX.

DISCUSSION

Despite the accumulating data on muscle SNA measured by microneurography in human studies, whether the neural discharge of muscle SNA correlates and coheres with that of other SNAs controlling visceral organs remains unclear. The major new findings in this study are (i) under the baroreflex closed-loop condition when CSP is matched with the systemic arterial pressure (CLOSE), muscle SNA resampled at 1 Hz correlates with both renal and cardiac SNAs in time-domain analysis (r^2: 0.6–0.7, with proper delay), and (ii) muscle SNA coheres with renal and cardiac SNAs in frequency domain analysis, particularly at peak frequencies of the SNA autospectra.

These results support our first hypothesis and indicate that muscle SNA correlates and coheres approximately with renal and cardiac SNAs under closed-loop baroreflex condition.

Next, although the baroreflex is known to strongly regulate muscles [3], renal and cardiac SNA [15, 20], the contribution of baroreflex to the homogeneous SNA discharges has not been elucidated quantitatively. The other major new findings in this study are as follows. When the change in baroreceptor pressure is increased from FIX (fixed CSP, no change) to CLOSE (CSP matching systemic arterial pressure, pulse pressure 30–40 mmHg) and further to WIDE (CSP fluctuating between ±40 mmHg), there are corresponding increases in the time domain correlation (r^2) of muscle SNA resampled at 1 Hz with renal and cardiac SNAs, from approximately 0.5 (FIX), to 0.6–0.7 (CLOSE), and to 0.8 (WIDE) (Fig. 5, A and B). The baroreflex dependent characteristics were also observed when SNAs were resampled at a frequency from 0.3 to 5.0 Hz (Fig. 6). This is also consistent with increases in the variance component of muscle SNA correlating with renal and cardiac SNAs (Fig. 5, C and D). These results agree with the concept that the baroreflex is important in generating harmonized SNA discharges [5, 21]. Moreover, the results indicate that arterial baroreflex has the ability to increase the homogeneity between these SNAs by nearly twofold. They support our second hypothesis and indicate that the arterial baroreflex potently homogenizes neural discharges of these SNAs.

Our results indicate that baroreflex increases the homogeneity between these SNAs by modulating SNA at nonpeak frequencies of SNA autospectra. The frequency domain correlation (coherence function) of muscle SNA with renal and cardiac SNAs was increased from approximately 0.4–0.5 (FIX), to 0.5 (CLOSE), to 0.9 (WIDE) at nonpeak frequencies, not peaking frequencies, of the SNA autospectra (Fig. 8). This suggests that other mechanisms other than baroreflex govern SNA at the nonpeak frequencies.

Our results quantitatively indicate that baroreflex-independent factors contribute to one-half of the homogeneity between muscle SNA and cardiac or renal SNA. Time-domain data show that even under a condition in which CSP is fixed at operating pressure, one-half of the variance of muscle SNAs correlates with other SNAs (Fig. 5, C and D; gray top column), with r^2 of approximately 0.5 (Fig. 5, A and B). These data indicate the presence of a baroreflex-independent component of SNA homogeneity. Although some noises may be included in the variance component of muscle SNA correlating with other SNAs, this is negligible in the calculation of variance, since the signal/noise ratio in SNA is >1,000 (noise was measured as the signal obtained after an individual animal died). The baroreflex-independent component of SNA homogeneity may be related to the strong coherence function between the SNAs at autospectral peak frequencies, since the coherence is consistently high regardless of the magnitude of baroreceptor pressure changes (Figs. 7, D and E, and 8). This component may partially be associated with the respiratory-related rhythm in sympathetic nerve discharge, a concept of central respiratory rhythm generator [21–23]. At the autospectral peak frequencies, these mechanisms may keep the coherence sufficiently high (0.9) independent of the baroreflex, and thus the baroreflex cannot increase the coherence further.

In contrast to the homogeneous sympathetic activation, the heterogeneity of muscle SNA versus renal or cardiac SNA does not relate with baroreflex. The proportions of the variance component of muscle SNA not correlating with renal and cardiac SNAs are constant regardless of the magnitude of change in baroreceptor pressure (Fig. 5, C and D). Mechanisms other than baroreflex may be involved in heterogeneous sympathetic activation. For example, chemoreflex [24], nitric oxide synthesis [25], and osmolarity [26] have been reported to produce regional differences in sympathetic activations.

Our data may strengthen the interpretation and the impact of the accumulated data on the involvement of human muscle SNA in circulatory physiology [3, 6–8, 10] and cardiovascular diseases [27, 28]. The recording of human microneurography is limited to the limbs, and there is so far little direct experimental evidence to support that muscle SNA parallel the other SNAs controlling visceral organs. The present study addresses this issue as an initial step and demonstrates the similarity between muscle SNA discharge and renal or cardiac SNA. Further study is needed to investigate the relations between SNAs in response to stimuli other than baroreflex.

Earlier studies have reported the coherence between pairs of SNA discharges for cardiac, renal, splanchnic, splenic, and lumbar SNAs in animals [29–31]. However, most of the studies focused on the coherence at frequencies faster than 1 Hz (0–15 Hz), in contrast to the present study. Furthermore, the previous studies did not measure muscle SNA or quantitatively investigate the effects of baroreflex on homogeneous SNA discharges.

Limitations

The present study has several limitations. First, anesthetic agents tend to inhibit efferent SNA and depress the gain of baroreflex control of SNA. Second, we excluded the efferent vagal nerve activities, which could affect SNA and baroreflex. Third, artificial respiration and surgical procedures used in this study may affect SNA and baroreflex. Last, based on most of the frequency domain studies of human muscle SNA [32–35], we focused on sympathetic discharge at frequencies of up to 1 Hz. And because of the low-pass characteristics of transfer function from SNA to arterial pressure (baroreflex peripheral arc) [20], the dynamic property of pressure response to